Binary Classification of Defective Solar PV Modules Using Thermography

Niazi, Kamran Ali Khan; Akhtar, Wajahat ; Khan, Hassan Abbas ; Sohaib, Sarmad ; Nasir, Ahmad Kamal

Published in:
Proceedings of the 2018 IEEE 7th World Conference on Photovoltaic Energy Conversion (WCPEC) (A Joint Conference of 45th IEEE PVSC, 28th PVSEC & 34th EU PVSEC)

Publication date:
2018

Binary Classification of Defective Solar PV Modules Using Thermography

Kamran Niazi[1,2], Wajahat Akhtar[3], Hassan Abbas Khan[1], Sarmad Sohaib[4], Ahmad Kamal Nasir[1]

1. Department of Electrical Engineering, SBA School of Science and Engineering, Lahore University of Management Sciences (LUMS), Lahore, Punjab, 54792, Pakistan

2. Department of Energy Technology, Aalborg University, Aalborg, Denmark

3. University of Heriot Watt, Edinburgh, UK

4. University of Engineering and Technology, Taxila, Pakistan

***Abstract*— Photovoltaic (PV) modules are subject to various internal or external stresses due to their operation in solar PV based power systems. Therefore, monitoring and maintenance are critical issues to ensure reliability of PV modules which in turn would affect the reliability of any PV system. In this paper, we categorize operational solar panels into two categories (Defective and Non-Defective panels) using a machine learning technique i.e. texture features through thermography assessment. Further, the panels are also categorized for diagnostic perspective using nBayes classifier. Results from an investigation for a 42.24 kWp PV system showed a mean recognition rate of 98.4% for a set of 260 test samples.**

***Index Terms*—PV solar panel, thermal imaging (TI), hotspots machine learning, nBayes classifier**

I. INTRODUCTION

Photovoltaic (PV) solar panel/module technology is now considered a key alternative for lowering carbon emissions [1]. However, the performance and efficiency of PV systems is affected by several factors which include shading, humidity, and wind [2-4]. In addition, there is also an effect of dust accumulation, and temperature on the performance of these panels with wide variations on the output power as reported in the literature [5, 6].

Faults in solar PV modules also increase with shading which can cause additional power losses [7, 8] and hotspots [9], thereby reducing power production and overall efficiency. Significant work is done to maximize the reliability and improve the maintainability of PV systems over the last few decades [10]. Image processing techniques are making continuous progress in biometric recognition [11, 12], robotic automation [13, 14] and industrial inspection [15-17]. These techniques along with machine learning algorithms can be used to find defects that develop on PV solar wafer and cell. For instance, cracks that appear at the edges of solar cells were detected by *Fu et al* [18] through machine vision method in solar PV cells by analyzing their geometric features. *Ordaz et al* [19] worked on solar cell based conversion efficiency by using gray-level distribution on electroluminescence (EL) images. However, this distribution method gives only the information of dark areas in the EL image without detecting local small defects.

While the available techniques allow identification of certain defects, there is an emerging need for Texture Feature Extraction (TFE) based automatic classification for solar PV panels. Available TFE based defect detection methods are applicable to non-textured or homogeneously textured surfaces detection. Therefore, in this work, we evaluate TFE-based approach for identification of solar PV panels as defective and non-defective. The proposed TFE-based model involves a machine learning technique to train the classifier. Initially, an inspection process for generation of the ground truth is conducted which act as true model for comparison. Each solar PV module image of both classes is first pre-processed, and a set of texture features are extracted creating feature descriptors for texture based binary image classification. Mean of each texture feature is computed at different angular directions to remove feature overlap to enhance features quality. A data matrix of all the quality features is created in a way that each image feature descriptor corresponds to one row of the data matrix. This data feature matrix is used to train the binary classifier (nBayes) with dataset of $k = 260$ images using a non-exhaustive K-fold leave-one-out cross validation training technique. At the end, testing is performed to compare each testing sample in the data with trained classifier.

II. METHODOLOGY

A flexible and modular framework (shown in Fig. 1) was developed which monitors and classifies solar PV panels by using feature extraction technique on thermal images (TIs) obtained from a thermal camera (FLIR Vue 640 pro). TI dataset was acquired from a 42 kW c-Si PV system [20] installed at Lahore University of Management Sciences (LUMS) and was examined by solar PV panel analysts. Investigation of the dataset was performed to split the dataset into two categories i.e. defective and non-defective. Preprocessing step was applied on each of the PV TI in dataset. Texture features descriptor was extracted to classify the testing thermal PV images into their respective categories. Overall a descriptor of 5 features was obtained from each image included; contrast, energy, homogeneity, correlation, and entropy given by (1) - (5), respectively.

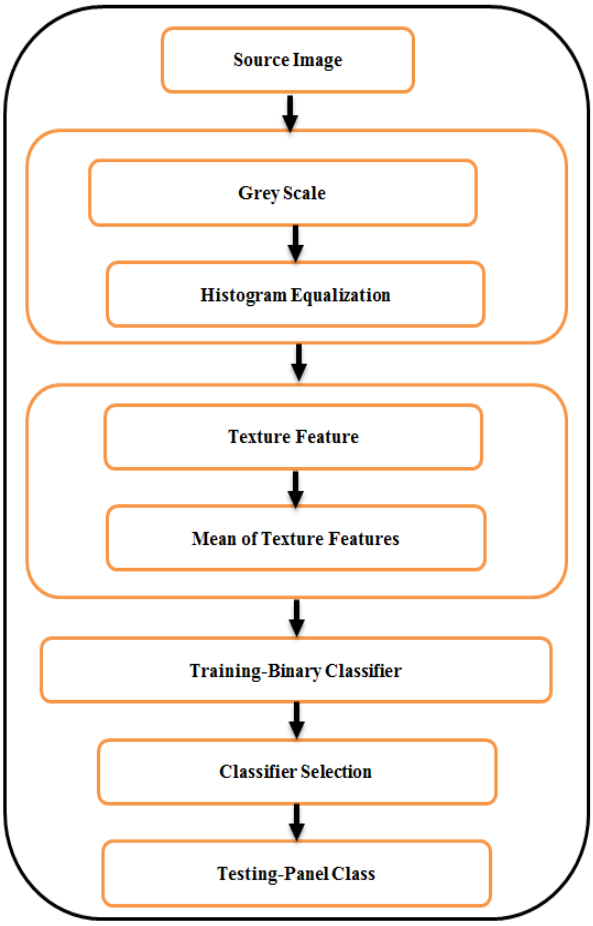

Fig.1. Block diagram of proposed feature based categorization of solar PV modules.

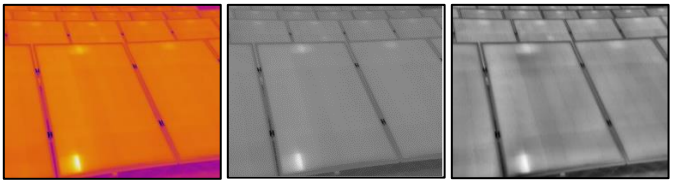

Fig.2 Prepossessed defective TI of PV panels (a) RGB image (b) gray scale (c) histogram equal.

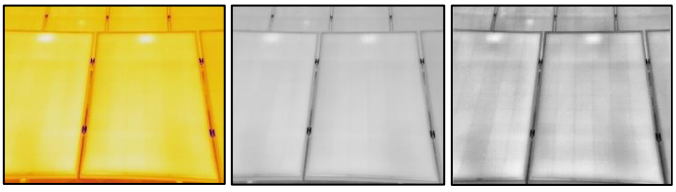

Fig. 3 Prepossessed non-defective TI of PV panels (a) RGB image (b) gray scale (c) histogram equal.

A. Data Acquisition and Ground Truth Generation

PV module TIs with a spatial resolution of 640×512 pixels were acquired using forward looking infrared camera. To generate the ground truth for training, the dataset was divided in to two classes namely defective and non-defective. Two solar PV panels analyst (registered electrical power engineers) from Pakistan Engineering Council were asked to manually label the acquired dataset. The two categories namely defective and not defective were made each containing 130 samples.

B. Preprocessing

Preprocessing was applied to improve the textural information and reliability of the collected data set of PV module TIs. It was used to remove measurement noise and artifacts appeared in PV panel TIs due to sensor measurements. Preprocessing steps for both classes i.e. defective and non-defective is shown in Fig. 2 and Fig. 3. TIs were first converted into gray scale to measure the intensity of light at each pixel in a single band of the electromagnetic spectrum as shown in Fig. 2(b) and Fig. 3(b). To further improve the contrast of the dataset, histogram equalization was applied [21] to all obtained converted gray scale PV module TIs as shown in Fig 2(c) and Fig. 3(c).

C. Feature Extraction

Texture features like contrast, correlation, energy, homogeneity, and entropy provide a complementary data that helps in classification of spectrally heterogeneous images in situations where spectral information is not adequately available. These were calculated from PV module TIs using gray level co-occurrence matrix (GLCM) [22]. The GLCM is a tabulation of how often different combinations of pixel brightness values (grey levels) occur in an image. Matlab's "graycomatrix" function was used to extract texture features which constructed the desired gray level GLCM. A 2D approach was followed where co-occurrence frequencies were calculated symmetrically for each of the preprocessed solar PV panel images with inter-sample space of five at four different angular directions (i.e. 0^o, 45^o, 90^o and 135^o) as shown in Fig. 4 (a-f) for defective while for non-defective in Fig. 5 (a-f). They were generated by computing local image features of window size 2x2. Initially, a descriptor of 20 features was computed at a sample space of 1. Mean of each texture feature at different angle was computed to further reduce the descriptor to five features (contrast, energy, homogeneity correlation, and entropy) for each of the angular directions to improve features quality and computational time. Features for inter sample space of 2, 3, 4 and 5 were also computed in a similar way as in case of sample space 1. Hence, each of the training data set image was used to extract a descriptor of size 25 features. The 5 important features are given by (1) - (5).

$$\text{Contrast} = \sum_{i,j=0}^{N-1} (i-j)^2 \times m_{ij} \quad (1)$$

$$\text{Energy} = \left(\sum_{i,j=0}^{N-1} m_{ij}^{\,2}\right)^{1/2} \quad (2)$$

$$\text{Homogeneity} = \sum_{i,j=0}^{N-1} \frac{m_{ij}}{1+|i-j|^2} \quad (3)$$

$$\text{Correlation} = \sum_{i,j=0}^{N-1} \frac{(i-\mu)\times(j-\mu)\times m_{ij}}{1+\sigma^2} \quad (4)$$

$$\text{Entropy} = \sum_{i,j=0}^{N-1} m_{ij} \times \log(m_{ij}) \quad (5)$$

where i, j represents the row and column number of the image, m_{ij} represent pixel location, $N-1$ is total number of rows and columns, μ is the mean and σ is the variance of the pixel value.

D. Training

A non-exhaustive K-fold leave-one-out cross validation technique was used to train the acquired dataset of $k = 260$ number of PV module TIs.

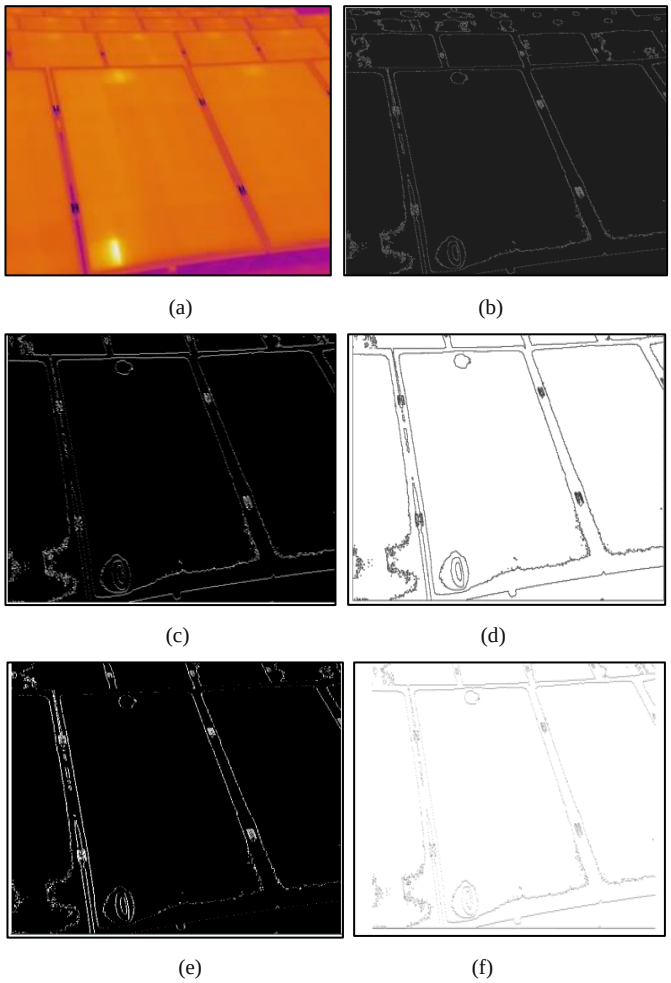

(a) (b) (c) (d) (e) (f)

Fig. 4 Defective (a) original image, (b) entropy, (c) contrast, (d) energy, (e) correlation, (f) homogeneity.

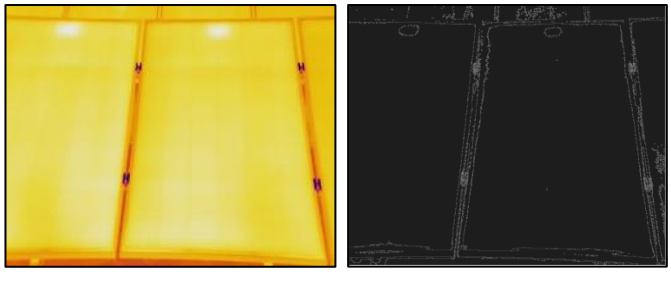

(a) (b)

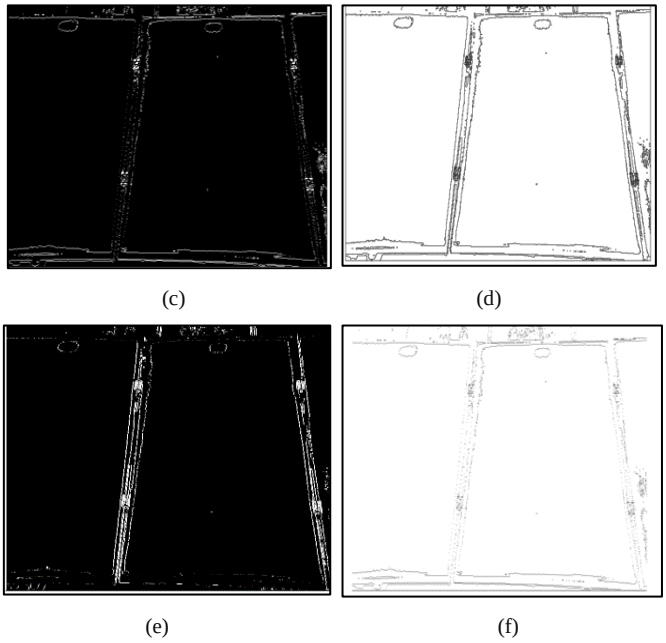

(c) (d) (e) (f)

Fig. 5 Non-defective (a) original image, (b) entropy, (c) contrast, (d) energy, (e) correlation, (f) homogeneity.

E. Classifier Selection

Matlab toolbox called PRTools is used for the classification as it offers many different user-friendly classifiers. PV module TIs were classified into two categories i.e. defective and non-defective. We used nBayes a binary class density based classifier which uses Bayes theorem to calculate explicit probability for each hypothesis [23].

III. Results and Experiments

Experimental results show that our proposed approach performed well in binary classification with a limited number of training samples. It is evaluated on the dataset of 260 PV module TIs. The model is trained with the proposed technique and the panels were classified into two respective classes i.e. defective and non-defective. Table I shows the mean intensity values of each texture feature computed at different angles for a sample image of class defective with inter-sample space 1. Table II shows the mean intensity values of each texture feature computed at different angle for an image of class non-defective with inter-sample space 1.

TABLE I
EXTRACTED FEATURES FOR SAMPLE DEFECTIVE IMAGE

Features	0^o	45^o	90^o	135^o	Mean value
Contrast	0.045	0.061	0.044	0.064	0.054
Energy	0.459	0.447	0.461	0.444	0.453
Homogeneity	0.977	0.969	0.977	0.967	0.973
Correlation	0.921	0.893	0.922	0.887	0.906
Entropy	0.856	0.856	0.887	0.887	0.871

TABLE II
EXTRACTED FEATURES FOR SAMPLE NON-DEFECTIVE IMAGE

Features	0°	45°	90°	135°	Mean value
Contrast	0.139	0.173	0.123	0.142	0.144
Energy	0.298	0.281	0.300	0.288	0.269
Homogeneity	0.955	0.940	0.958	0.947	0.928
Correlation	0.899	0.875	0.911	0.898	0.896
Entropy	0.838	0.854	0.759	0.852	0.825

The mean intensity values in table I and II clearly depict that all the texture feature plays a vital role in helping the classifier to categorize the images into their respective classes especially in case of contrast, energy, homogeneity and entropy.

TABLE III
SYSTEM PERFORMANCE

Section	Class 1	Class 2	Model Accuracy
Sensitivity	0.9692	1	0.984
Specificity	1	0.969	
Precision	1	0.970	

TABLE IV
CONFUSION MATRIX

Section	Predicted Classes		
Actual Classes	Categories	Class 1	Class 2
	Class 1	126	4
	Class 2	0	130

Suggestion of predictive maintenance measure was necessary for each category of the defect which makes the system intelligent by minimizing the PV power losses and maximizes its output. Model accuracy, sensitivity, specificity and precision of the proposed system of each class are summarized in Table III. Outcome of proposed classification method is also formulated in 2x2 confusion matrix (see Table IV). The diagonal integer values in Table IV depicts correct classification of PV TIs for all the classes from 260 test sample images (i.e. 256 images), with 4 misclassified predicted PV TIs. It is evident that the probability of each testing PV panel TI lying in a specific class was found to be very high. This results in proper classification of panels in their respective classes. Table III and IV shows that the proposed model achieved a remarkable high precision and sensitivity (true positive rate), therefore, classifying most of the PV panels correctly. The model accuracy achieved is 98.4% for a set of combined 260 test samples of defective and non-defective PV module TIs using leave-one-outcross validation method.

IV. CONCLUSION

In this paper, we have developed a flexible thermal imaging based framework that can automatically perform binary classification of solar PV panel into defective and non-defective. It has high model accuracy of 98.4 % with high precision and sensitivity values. This model has allowed us to test and evaluate many different approaches and configurations that could be used in real time on different systems with very low computational time.

REFERENCES

[1] P. Y. Gan and Z. Li, "Quantitative study on long term global solar photovoltaic market," *Renewable and Sustainable Energy Reviews,* vol. 46, pp. 88-99, 2015.

[2] J. K. Kaldellis, M. Kapsali, and K. A. Kavadias, "Temperature and wind speed impact on the efficiency of PV installations. Experience obtained from outdoor measurements in Greece," *Renewable Energy,* vol. 66, pp. 612-624, 2014.

[3] R. Eke and T. R. Betts, "Spectral irradiance effects on the outdoor performance of photovoltaic modules," *Renewable and Sustainable Energy Reviews,* vol. 69, pp. 429-434, 2017.

[4] M. Dhimish and V. Holmes, "Fault detection algorithm for grid-connected photovoltaic plants," *Solar Energy,* vol. 137, pp. 236-245, 2016.

[5] M. Saidan, A. G. Albaali, E. Alasis, and J. K. Kaldellis, "Experimental study on the effect of dust deposition on solar photovoltaic panels in desert environment," *Renewable Energy,* vol. 92, pp. 499-505, 2016.

[6] M. A. Ramli, E. Prasetyono, R. W. Wicaksana, N. A. Windarko, K. Sedraoui, and Y. A. Al-Turki, "On the investigation of photovoltaic output power reduction due to dust accumulation and weather conditions," *Renewable Energy,* vol. 99, pp. 836-844, 2016.

[7] A. Maki and S. Valkealahti, "Effect of photovoltaic generator components on the number of MPPs under partial shading conditions," *IEEE Transactions on Energy Conversion,* vol. 28, no. 4, pp. 1008-1017, 2013.

[8] E. V. Paraskevadaki and S. A. Papathanassiou, "Evaluation of MPP voltage and power of mc-Si PV modules in partial shading conditions," *IEEE Transactions on Energy Conversion,* vol. 26, no. 3, pp. 923-932, 2011.

[9] M. S. El-Dein, M. Kazerani, and M. Salama, "Optimal photovoltaic array reconfiguration to reduce partial shading losses," *IEEE Transactions on Sustainable Energy,* vol. 4, no. 1, pp. 145-153, 2013.

[10] H. A. Lauffenburger and R. T. Anderson, "Reliability terminology and formulae for photovoltaic power systems," *IEEE Transactions on reliability,* vol. 31, no. 3, pp. 289-295, 1982.

[11] Y. Si, J. Mei, and H. Gao, "Novel approaches to improve robustness, accuracy and rapidity of iris recognition systems," *IEEE Transactions on Industrial Informatics,* vol. 8, no. 1, pp. 110-117, 2012.

[12] S. Jin, D. Kim, T. T. Nguyen, D. Kim, M. Kim, and J. W. Jeon, "Design and implementation of a pipelined datapath for high-speed face detection using FPGA," *IEEE Transactions on Industrial Informatics,* vol. 8, no. 1, pp. 158-167, 2012.

[13] R. Gerndt, S. Michalik, and S. Krupop, "Embedded vision system for robotics and industrial automation," in

Industrial Informatics (INDIN), 2011 9th IEEE International Conference on, 2011, pp. 895-899: IEEE.

[14] S. Livatino, F. Banno, and G. Muscato, "3-D integration of robot vision and laser data with semiautomatic calibration in augmented reality stereoscopic visual interface," *IEEE Transactions on Industrial Informatics*, vol. 8, no. 1, pp. 69-77, 2012.

[15] C.-h. Chan and G. K. Pang, "Fabric defect detection by Fourier analysis," *IEEE transactions on industry applications*, vol. 36, no. 5, pp. 1267-1276, 2000.

[16] A. Picón, O. Ghita, P. F. Whelan, and P. M. Iriondo, "Fuzzy spectral and spatial feature integration for classification of nonferrous materials in hyperspectral data," *IEEE Transactions on Industrial Informatics*, vol. 5, no. 4, pp. 483-494, 2009.

[17] D.-M. Tsai, I.-Y. Chiang, and Y.-H. Tsai, "A shift-tolerant dissimilarity measure for surface defect detection," *IEEE Transactions on Industrial Informatics*, vol. 8, no. 1, pp. 128-137, 2012.

[18] F. Zhuang *et al.*, "Solar cell crack inspection by image processing," in *Business of Electronic Product Reliability and Liability, 2004 International Conference on*, 2004, pp. 77-80: IEEE.

[19] M. A. Ordaz and G. B. Lush, "Machine vision for solar cell characterization," in *Proceedings of SPIE*, 2000, vol. 3966, pp. 238-248.

[20] A. S. Rana, M. Nasir, and H. A. Khan, "String level optimisation on grid-tied solar PV systems to reduce partial shading loss," *IET Renewable Power Generation*, Available: http://digital-library.theiet.org/content/journals/10.1049/iet-rpg.2017.0229

[21] K. Zuiderveld, "Contrast limited adaptive histogram equalization," in *Graphics gems IV*, 1994, pp. 474-485: Academic Press Professional, Inc.

[22] F. Albregtsen, "Statistical texture measures computed from gray level coocurrence matrices," *Image processing laboratory, department of informatics, university of oslo*, vol. 5, 2008.

[23] M. J. Islam, Q. J. Wu, M. Ahmadi, and M. A. Sid-Ahmed, "Investigating the performance of naive-bayes classifiers and k-nearest neighbor classifiers," in *Convergence Information Technology, 2007. International Conference on*, 2007, pp. 1541-1546: IEEE.